Colloid Polym Sci 273:886–892 (1995)
© Steinkopff Verlag 1995

ORIGINAL CONTRIBUTION

J. Tanori
N. Duxin
C. Petit
I. Lisiecki
P. Veillet
M.P. Pileni

Synthesis of nanosize metallic and alloyed particles in ordered phases

Received: 25 January 1995
Accepted: 17 March 1995

J. Tanori · N. Duxin · C. Petit
I. Lisiecki · Prof. M.P. Pileni (✉)
Université Pierre et Marie Curie
Laboratoire "Structure et Réactivité des Systèmes Interfaciaux"
URA CNRS 1662
BP 52
4 place Jussieu
75005 Paris, France

J. Tanori · N. Duxin · C. Petit
I. Lisiecki · M.P. Pileni
CEA-DSM-DRECAM Service de Chimie Moléculaire
CE Saclay
91191 Gif sur Yvette, Cedex, France

P. Veillet
Institut d'Electronique Fondamentale
URA CNRS 22
Centre Universitaire d'Orsay, Bât. 220
91405 Orsay Cedex, France

Abstract Functionalized reverse micelles have been used to synthesize Copper and Cobalt nanoparticles differing by their size and shape. They can be also used to synthesize Fe-Cu alloy (at 30% Fe) and composite (at 70% Fe) particles. In the case of Fe-Cu system, the magnetic properties are presented.

Key words Nanoparticles iron – copper – cobalt – alloys

Introduction

Nanosized particles of metal and alloys exhibit properties which drastically differ from the bulk [1]. The possibility to prepare ultrafine particles with homogeneous morphology and size would be of great interest in the technological [2] (magnetic recording) and theoretical [3] (quantum size effect) fields.

Sodium di-(ethyl hexyl sulfosuccinate) (NaAOT), -isooctane-water solution forms water in oil droplets characterized by a size which varies linearly with the water content, $w = [H_2O]/[AOT]$ [4]. The synthesis of solid particles in water, by ion reduction or by the formation of an insoluble salt, can be controlled by the size of the water droplets in which it takes place [5–7].

In this paper, the production of metallic copper particles by reduction of copper(II) ions in some surfactant mesophases is reported. It is shown that the size and the shape of the copper particles depend on the mesophase structure where the chemical reaction occurs. Formation of nanosized cobalt particles is observed with a decrease in the size by increasing the water content. Fe-Cu alloys are obtained by addition of a large amount of water containing a reducing agent such as sodium borohydride to the mixed micellar solution.

Experimental section

Synthesis-metallic particles have been performed by using metal (II) bis(2-ethylhexyl) sulfosuccinate [$Cu(AOT)_2$, $Co(AOT)_2$ or $Fe(AOT)_2$]-water-isooctane. The preparation of the copper, iron and cobalt surfactants has been described previously [8]. All the particles were synthesized under a N_2 atmosphere. Isooctane was supplied by Fluka (99.5% puriss), hydrazine (100%) by Merck, sodium borohydride by Sigma and single distilled water was passed through a Millipore "MilliQ" system cartridge until its resistivity reached 18 MΩ·cm. All chemicals were used without further purification.

Transmission electron microscopy and the electron micrographs were obtained with a Jeol electron microscope (model Jem. 100 CX.2).

The electrical conductivity measurements were made with a Tacussel CD 810 instrument using a TD 100 (platinum) electrode from the same manufacturer. The measurements were made at 25 °C once a stable reading had been established.

Magnetic studies are done with a commercial alternative gradient magnetometer operating at room temperature in a field up to 2 Teslas.

Syntheses

Synthesis of copper particles

i) In mixed reverse micelles

The preparation of colloidal copper particles is achieved by mixing the reverse micellar system with an aqueous solution of hydrazine. The quaternary system is used: $Cu(AOT)_2$–Na(AOT)-water-isooctane. The reverse micellar solution are formed by solubilizing an AOT micellar solution containing copper bis (2-ethylhexyl)sulfosuccinate surfactant, $Cu(AOT)_2$, 10^{-2} M, with sodium (2-ethylhexyl)sulfosuccinate surfactant, Na(AOT), 0.08 M. Hydrazine is the reducing agent $[N_2H_4] = 3\ 10^{-2}$ M. A change in the water content of the micelle, w $(1 < w < 15)$, is obtained by adding H_2O to the micellar solution before the reaction takes place.

ii) In pure $Cu(AOT)_2$/water/isooctane system

Hydrazine, $[N_2H_4] = 0.15$ M, used as a reducing agent, is added to solution containing copper AOT $\{[Cu(AOT)_2] = 5.10^{-2}$ M$\}$. A change in the water content of the micelle, w, or in shape is obtained by adding H_2O to the solution before the reaction takes place. In all the cases, particular care was taken to prevent oxidation of the particles and electron diffraction of clusters does indeed show rays characteristic of metallic copper

Synthesis of cobalt particles

The synthesis of cobalt nanoparticles is carried out in quaternary system: Na(AOT)-$Co(AOT)_2$-water-isooctane; using sodium borohydride as reducing agent $[NaBH_4] = 4{\cdot}10^{-3}$ M, with $[Co(AOT)_2] = 10^{-3}$ M and [Na(AOT)] = 0·25 M. Reducing agent is added as aqueous solution, in deoxygenated reverse micelle solution at different water-contents, w. $(2.5 < w < 20)$.

Synthesis of Fe-Cu alloys particles

When a 0.1 M of $Fe(AOT)_2$-$Cu(AOT)_2$-isooctane micellar solution is added to an equal volume of a 0.2 M $NaBH_4$ aqueous under vigorous stirring, a black precipitate appears. It is washed first with isooctane and then with acetone to remove all the surfactant. The precipitate is then dried in an Ar atmosphere chamber. This experiment has been performed from reverse micelles containing 30% of iron and 70% of copper derivatives and vice versa.

Results and discussion

Copper metallic particles: Change in size and shape

Phase progression with increasing water content

In the quaternary system, $Cu(AOT)_2$-NaAOT-water-isooctane, an isotropic solution is obtained. It is characterized by a very low conductivity (less than 100 nS). It has been demonstrated by SAXS experiments [8], the formation of water in oil droplets with a radius unchanged compared to Na(AOT)-water-isooctane reverse micelles. Hence, the water pool radius increases with the water content as $R_w = 1.5\ w$ [9]. The $Cu(AOT)_2$ and NaAOT concentration used are equal to $2{\cdot}10^{-2}$ M and $8{\cdot}10^{-2}$ M, respectively.

The phase progression of the ternary system, $Cu(AOT)_2$-water-isooctane, strongly depends on the water content, w. The behavior of the phase diagram, described below, is given for a $Cu(AOT)_2$ concentration equal to $5{\cdot}10^{-2}$ M.

At low water content (below $w = 5$), an isotropic solution is observed characterized by a low conductivity (about 20 nS). From SAXS [8], it has been demonstrated that below $w = 3$, spherical droplets ($w = 2.5$, $r = 1.2$ nm) are formed, whereas above $w = 3$ the droplets are elongated with a cylindrical structure. This solution is usually called L_2 phase.

At $w = 5.5$, the L_2 solution is destabilized with the appearance of a phase transition. The upper phase is pure isooctane and all the surfactant is located in the lower phase. By increasing the water content from $w = 5.5$ to 9.5, the volume of the upper phase increases which induces an increase in the surfactant concentration of the lower phase. As the lower phase becomes more concentrated, the conductivity drastically increases from 60 to 1200 μS. Such a strong increase in the conductivity and surfactant concentration with the water content indicates a bicontinuous structure with an interconnected network. The lower phase is called $L_2(I)$ phase.

At $w = 9.8$, a third, turbid and birefringent phase appears between the isooctane and $L_2(I)$ phase. By increasing the water content from 10 to 14, the volume of the new phase progressively increases, whereas the $L_2(I)$ phase disappears. This third phase is a lamellar phase usually called $L(\alpha)$. Thus between $w = 10$ and 14, three phases ($L_2(I)$, $L(\alpha)$ and isooctane phases) are in equilibrium.

At $w = 14$, the $L_2(I)$ phase totally disappears, only $L(\alpha)$ and isooctane exist further. The conductivity of the $L(\alpha)$ phase, at $w = 14$, is very low (7.27 μS) compared to the $L_2(I)$ phase (1200 μS) at $w = 9.5$. This confirms a decrease in the degree of interconnection as it is usually observed in the lamellar phase [10]. $L(\alpha)$ phase consists of thin aqueous and thick isooctane lamellae.

At $w = 16$, a new isotropic phase appears in coexistence with $L(\alpha)$ and isooctane phases. With increasing water content the amounts of $L(\alpha)$ and isooctane decrease and that of the isotropic phase called $L_2(II)$ phase increases. From $w = 16$ to $w = 20$, the conductivity of the $L_2(II)$ phase decreases from 700 to 450 μS progressively. SAXS indicates spherical droplets the radius of which increases with the water content as it has been demonstrated for the Na(AOT)-water-isooctane system [9].

At $w = 20$, $L(\alpha)$ phase totally disappears and the $L_2(II)$ and isooctane phases remain in equilibrium. By increasing the water content from $w = 20$ to 30, the volume of the upper phase decreases and that of the $L_2(II)$ phase increases.

At $w = 30$, an isotropic solution is created. The radius of the water in oil droplets, derived from SAXS is 5.2 nm.

Synthesis of pure metallic copper nanocrystallites

Change in the particle size

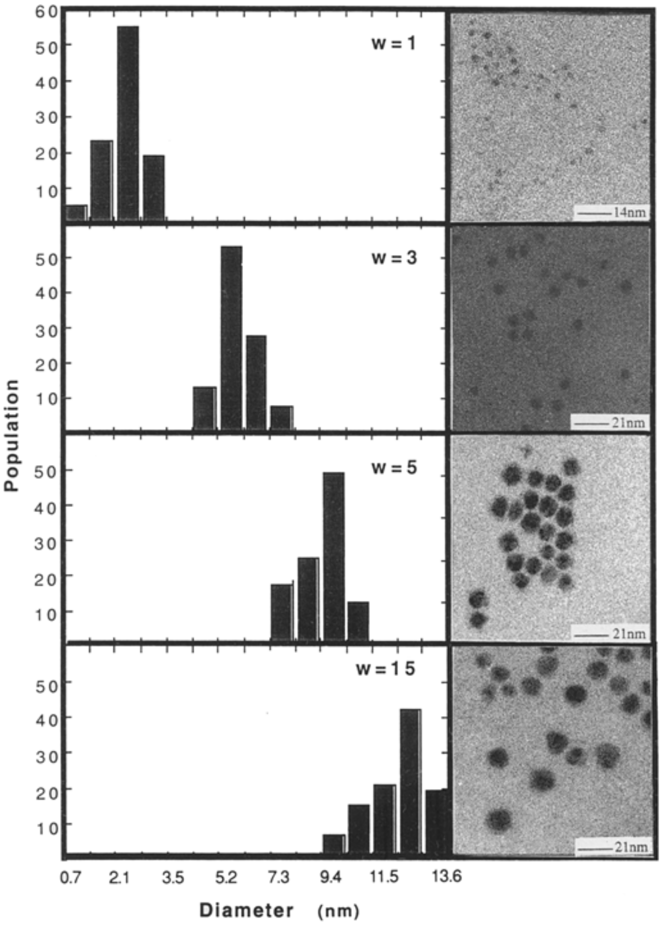

Fig. 1 Electron microscopy and histograms of metallic copper particles prepared in reverse micelles with various water contents: [AOT] = 0.1 M; $[Cu(AOT)_2] = 10^{-2}$ M; $[N_2H_4] = 2 \times 10^{-2}$ M

The electron microscopy picture (Fig. 1) shows an increase in the size of the particles from 2 to 12 nm with increasing water content from 1 to 10. At a water content above 10, the size of the particles remains unchanged but the polydispersity increases. Electron diffractograms, obtained at various water contents, are in good agreement with a simulated diffractogram of bulk metal copper. This indicates a crystalline face-centered cubic structure (f.c.c.) with a lattice constant of 3.61.

The change in the particle size with water content can be explained in terms of interfacial water structure: at low water content, copper ions are not fully hydrated and the effective number of ions participating in the chemical reduction is small. With the water content, the number of copper ions increases which react with hydrazine. This favours the growth of the metallic particles. At relatively high water content (above 10), copper ions in the droplets are fully hydrated and free water molecules are present [11]. This favors diffusion of copper ions into the droplet. Electrostatic interactions between the head polar groups of the surfactant and copper ions compete with hydration energy. The difference in these energies remains constant upon increasing the water content which keeps the particle size constant. An increase in the polydispersity with the water content could be attributed to a decrease in interfacial rigidity [12].

Change in the particle shape

Synthesis performed at $w = 4$ in homogeneous reverse micellar solution (the L_2 phase) induces the formation of spherical pure metallic copper particles with an average radius of 10 nm (Fig. 2A). However, small amounts of cylindrical particles are also observed. We must remember that, in this phase, the synthesis occurs in cylindrical water in oil droplets.

At $w = 5.6$, corresponding to the $L_2(I)$ phase in equilibrium with pure isooctane, the number of cylindrical metallic copper particles strongly increases, whereas the number of spherical crystallites decreases. The average size of the cylinders is 19 nm long with a diameter of 7 nm, whereas the average diameter of the spheres is equal to 10 nm (Fig. 2B).

At $w = 9.8$, where the $L(\alpha)$ phase appears, rod-like metallic copper particles are observed (Fig. 3) which are much larger than the particles sizes obtained in L_2 and $L_2(I)$ phases. As a matter of fact, the diameter of these particles varies from 10 to 30 nm and the length from 300 to 1500 nm.

At $w = 20$, when the $L_2(III)$ phase forms, spherical nanosized particles are produced with an average diameter equal to 10 nm (Fig. 2C).

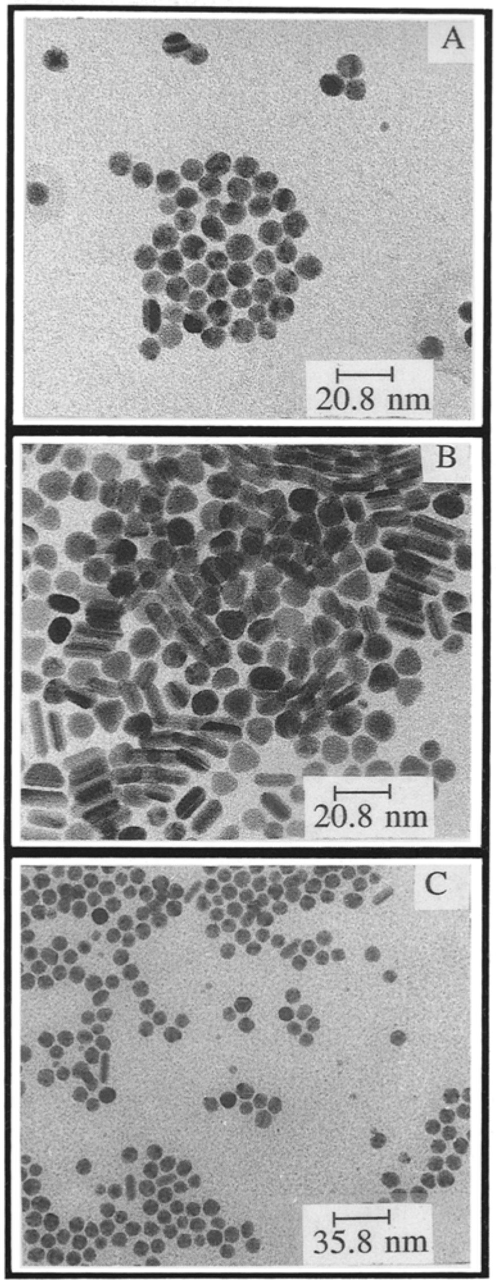

Fig. 2 Electron micrograph of metallic copper particles prepared in a reverse micellar solution L_2. (**A**), $L_2(I)$ (**B**) and $L_2(III)$ (**C**) phases

Cobalt nanoparticles: Change in size

For pure cobalt metallic particles there is a monotonous absorption spectrum from 250 nm to 800 nm [13]. In the case of cobalt oxide, a maximum in the absorption spectrum is observed around 350 nm without any absorption at 650 nm [14] (insert Fig. 4).

The absorption spectra after addition of $NaBH_4$ are recorded in Fig. 4:

At low water content ($w \leq 2.5$) the black-brown solution, characteristic of pure cobalt particles, does not appear. This is probably due to a low dissociation of the cobalt and BH_4^- ions from their counterions at this low water-content.

By increasing the water content, $2.5 \leq w \leq 7.5$, the characteristic absorption spectrum of cobalt particles appears.

At $w = 10$, the absorption at 650 nm is slightly weaker than at $w = 7.5$, a shoulder appears at 350 nm which is attributed to oxide derivate. This effect increases with the water content ($w = 20$).

Transmission Electron Microscopy and size histograms (Fig. 5) show a decrease in the cobalt particle size by increasing the water content from 6.3 nm at $w = 5$ to 3 nm in diameter at $w = 10$. The electron diffraction patterns are

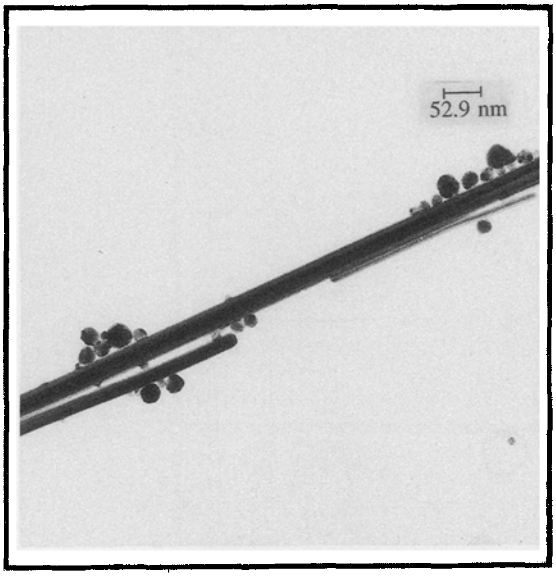

Fig. 3 Electron micrographs of copper rods prepared in lamellar phases L_α

Fig. 4 Absorption spectra of cobalt particles prepared at different water contents. [AOT] = 0.25 M in isooctane. $[Co(AOT)_2] = 10^{-3}$ M. $[NaBH_4] = 4 \cdot 10^{-3}$ M. Insert shows the characteristic spectrum of cobalt particles after reoxygenation ($W = 7.5$ in isooctane)

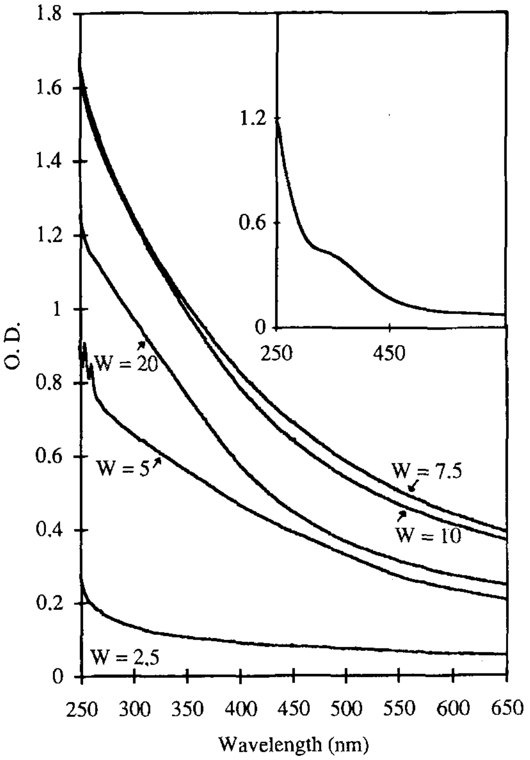

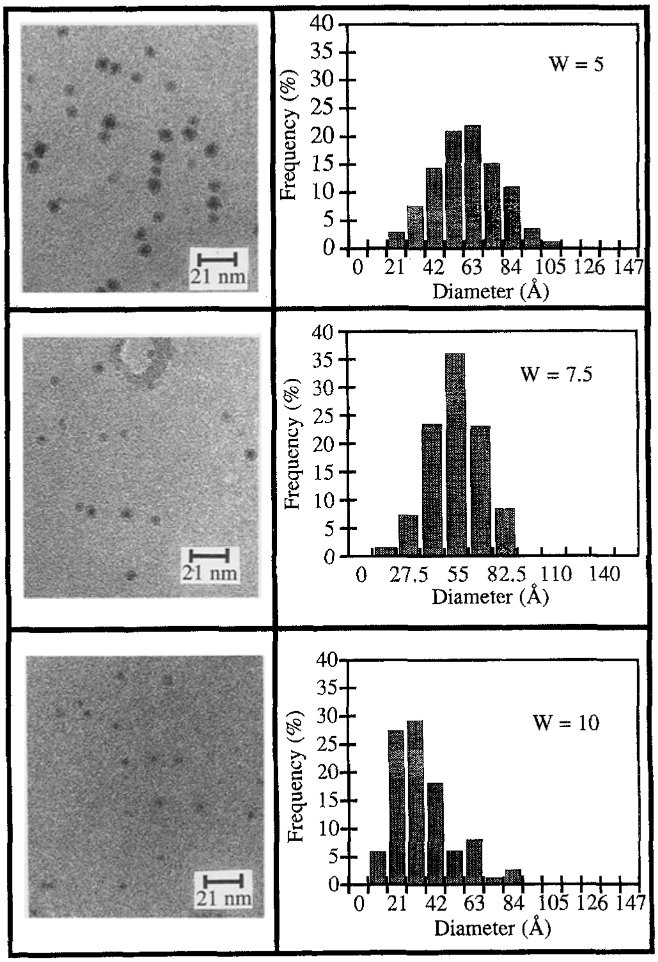

Fig. 5 Transmission electron microscopy and histograms of size of cobalt particles prepared at different water contents. [AOT] = 0.25 M in isooctane. $[Co(AOT)_2] = 10^{-3}$ M. $[NaBH_4] = 4 \cdot 10^{-3}$ M

characteristic of hexagonal cobalt particles. However, the presence of boride derivatives Co_2B or metaborates surrounding the particles cannot be totally excluded [14]. Increasing the water content decreases the particle size and cobalt oxide is formed. Similar behavior has been observed in the synthesis of copper metallic particles made with sodium borohydride as reducing agent [7]. At low water content pure and large metallic particles are formed. By increasing the water content, the size of particle decreases with formation of shell of oxide. Evidently, the oxide shells prevent the growth of the particles.

Fe-Cu: Ultrafine powders of alloy and composite

The microanalysis of the precipitate indicates that the particles retain the same ratio of iron and copper as in the solution. In both cases, x-rays diffraction shows a FCC structure of metallic and oxide copper particles while the BCC structure of the α-Fe phase is not detected. Transmission Electron Micrographs show particles with diameter of about 6 nm for 30%-iron (Fig. 6A) and 15 nm for 70%-iron (Fig. 6B). These small particles aggregate in larger particles.

The magnetization curves at room temperature of the two samples (30% Fe–70% Cu and 70% Fe–30% Cu) are strongly different. The 30% Fe–70% Cu sample is characterized by a very small coercive field (20 Oe) and a saturation moment of 103 kA/m (Fig. 7A). By annealing at 200 °C for 12 h in an Ar atmosphere, the magnetization curve changes (Fig. 7B). The coercive field increases from 20 to 380 Oe, but the saturation moment changes only slightly (from 103 to 112 kA/m). These changes could be due either to changes of the internal structure by a beginning phase separation or by grain growth.

In the case of 70% Fe–30% Cu, saturation is reached at 5000 Oe and a larger coercivity (220 Oe) is observed (Fig. 7C). After annealing, the coercivity does not strongly change, but the saturation moment increases (Fig. 7D).

In both samples, the saturation moment is small in regard to the iron content (the bulk saturation moment of iron is 1710 kA/m [15]): about 560 kA/m for 30% Fe–70% Cu and about 1200 kA/m for 70% Fe–30% Cu. The small saturation value could be due to the small size of the particles which yields to a superparamagnetic behavior and/or to the presence of oxide in the sample.

As it has been already described in the literature [16], the difference in the magnetic behavior between the two

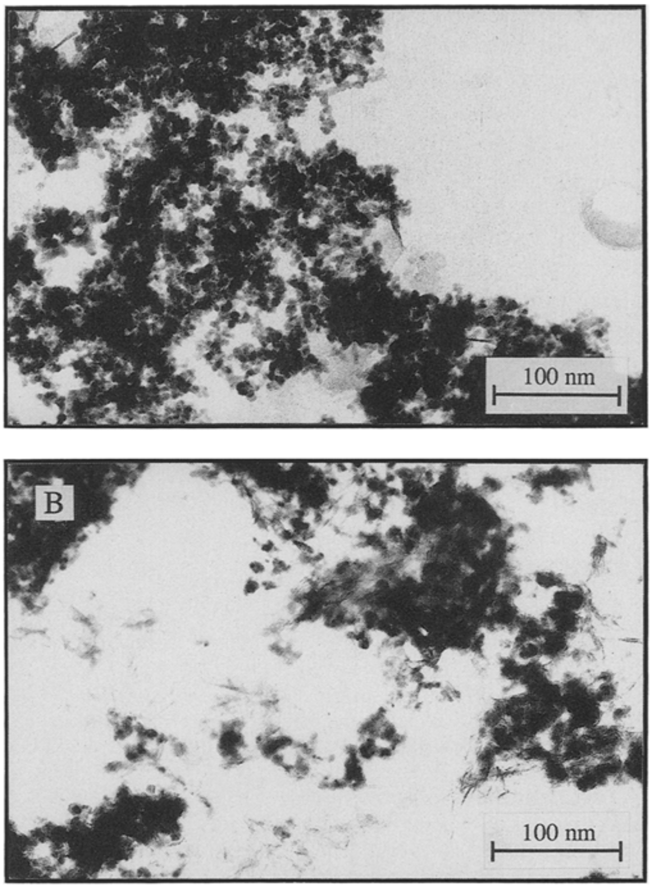

Fig. 6 Transmission electron microscopy of 30% Fe–70% Cu (A) and 70% Fe–30% Cu (B) particles

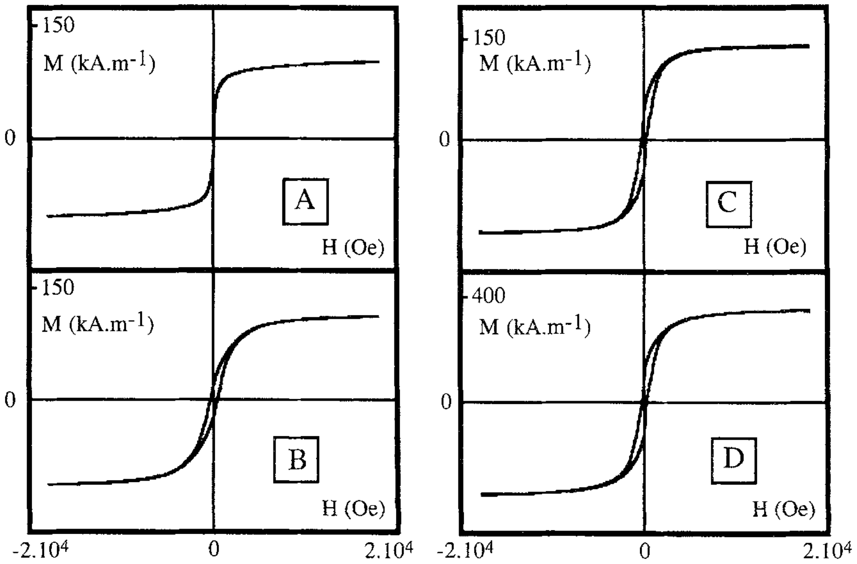

Fig. 7 Magnetization plots of 30% Fe–70% Cu before (A) and after (B) annealing and 70% Fe–30% Cu before (C) and after (D) annealing

samples could reflect changes in the structure of the particles. The low coercivity of the 30% Fe–70% Cu sample is characteristic of the Fe–Cu alloys. The larger coercivity observed with 70% Fe–30% Cu is characteristic of a composite material. It has to be noticed that the composition of the powder by x-ray microanalysis is the same as expected from the ratio of the components for the synthesis. However, in the x-ray diffraction of 70% Fe–30% Cu, the BCC structure of α-Fe phase is not obtained. This could be partially due to the presence of borate and oxide in the system or to small and amorphous iron particles as suggested by Transmission Electron Microscopy (Fig. 6B).

Conclusion

A correlation has been shown between the structure of the mesophase in the surfactant system with the size and the shape of the formation of pure copper metallic particle.

We have used functionalized surfactant to synthesize cobalt nanoparticle. The size of cobalt particles decreases with the water content as a consequence of the formation of oxide shell which prevent the particle growth.

Nanopowders of Fe-Cu alloys are formed. The magnetic values strongly change with composition, which could be due to internal structural changes.

References

1. Siegel R (1993) NanoStructured Materials 3:1
2. Bate G (1992) J Magn Magn Mater 100:413–421
3. Awschalom DD, DiVincenzo DP, Smyth JF (1992) Science p 258
4. Pileni MP (ed) Structure and reactivity in reverse Micelles. Elsevier, Amsterdam
5. Motte L, Petit C, Boulanger L, Lixon P, Pileni MP (1992) Langmuir 4:1049
6. Petit C, Lixon P, Pileni MP (1993) J Phys Chem 97:12975
7. Lisiecki I, Pileni MP (1993) J Amer Chem Soc 115:3887
8. Petit C, Lixon P, Pileni MP (1990) J Phys Chem 94:1598
9. Pileni MP, Zemb T, Petit C (1985) Chem Phys Lett 118:414
10. Petit C, Zemb Th, Pileni MP (1991) Langmuir Vol 7 No 2; 223
11. Haandrikman G, Daane GJR, Kerkohf FIM, va Os NM, Ruppert LAM (1992) J Phys Chem 96:9061
12. Truong VV, Scott GD (1977) J Opt Soc Am 67:502
13. Mie G (1908) Ann d Physik 25:377
14. Corrias A, Ennas G, Musinu A, Marongiu G, Paschina G (1993) Chem Mater 5:1722
15. "Magnetsim and Mettallurgy of Soft Magnetic Materials", Chen CW; Selected Topics in Solid State Physics, Wohlfarth EP. Ed, Vol XV, North Holland Publishing (1977)
16. Chow GM, Ambrose T, Xiao JQ, Twigg ME, Baral S, Ervin AM, Qadri SB, Feng CR (1992) Nanostructured materials (1992) 1:361